Journal of Engineering Physics and Thermophysics, Vol. 77, No. 5, 2004

INFLUENCE OF TURBULENCE ON THE DEPOSITION OF PARTICLES FROM A GAS-DISPERSED FLOW ON THE WALL

K. N. Volkov

UDC 532.529:536.24

Simulation of the scattering and deposition of dispersed-phase particles in the region of interaction of a turbulent flow with an obstacle is considered. The regimes and distinctive features of deposition of particles in the vicinity of a critical point are investigated under different conditions. The sedimentation coefficient of the impurity is calculated as a function of the parameters of unperturbed flow and the particle size. The results of the calculations are compared to the data obtained without allowance for the influence of the fluctuations of the carrier-flow velocity on the motion of the impurity.

Introduction. The problem on the influence of different factors on the deposition of an impurity from a gas-dispersed flow on the wall is of interest for many applications. In practice, the deposition of an impurity is both useful (in gas-thermal spraying of coatings and in gas-cleaning systems and measuring devices) and harmful (slagging of pipelines, disruption of IC production) in character. In many cases intensification of the transport properties of a medium and increase in the degree of deposition of an impurity on the wall are linked to the turbulent character of the flows formed.

Actual technical devices are characterized by the formation of small-scale gasdynamic singularities (stagnation zones, regions of separation or reattachment of the flow) caused by different structural members or flow-rate factors, which leads to localized precipitation of the condensed phase and becomes the reason for the local increase in heat transfer and other intensifying mechanisms that have an effect on the operating capacity and longevity of the structure.

The deposition of particles from a turbulent flow on the wall is due to the action of different factors and mechanisms (inertial, diffusional, thermophoretic, gravitational, centrifugal, and others), and theoretical models of deposition of an impurity differ by the adopted principal driving force of the process [1]. In free-inertial models, it is assumed that particles arrive at the wall due to their ejection from wall turbulent vortices. Convective-inertial models link the process of deposition of particles to the inertial effects in ingress of large vortices into the boundary layer [2]. Diffusion models are based on the assumption that in the wall region, the coefficient of turbulent diffusion of a dispersed phase exceeds the coefficient of turbulent diffusion of a carrier gas due to the inertia of particles [3]. In migration models, the turbulent movement of particles (turbophoresis) to the wall because of the fluctuations of the carrier-flow velocity is taken into account [4, 5].

The available data show that there is a certain critical value of the Stokes number Stk_* separating the regimes of impurity motion in which the deposition of particles on the obstacle surface exists or is absent [6, 7]. With the use of the singular-perturbation theory, it has been shown that the cases of the presence ($\mathrm{Stk} > \mathrm{Stk}_*$) or absence ($\mathrm{Stk} < \mathrm{Stk}_*$) of the inertial deposition of an impurity differ in the conditions of asymptotic join of the solution in the internal viscous region (in the boundary layer) with the external nonviscous solution [8].

The influence of the nonequilibrium of the flow in front of the shock wave on the sedimentation coefficient of particles in the vicinity of a critical point is investigated in [9]. The problem on the relation of the temperature of the surface in flow to the inertial deposition of an impurity is considered in [7, 10]. As a result of the numerical experiments carried out in the range of the temperature factor ϑ_w = 0.4–2, the coefficient of sedimentation of an impurity on the surface of a sphere as a function of the particle size has been obtained [10]. When $r_p > r_{p*}$ all the $\zeta(r_p)$

D. F. Ustinov Baltic State Technical University (VOENMEKh), 1 1st Krasnoarmeiskaya Str., St. Petersburg, 190005, Russia; email: dsci@mail.ru. Translated from Inzhenerno-Fizicheskii Zhurnal, Vol. 77, No. 5, pp. 20–28, September–October, 2004. Original article submitted November 20, 2003.

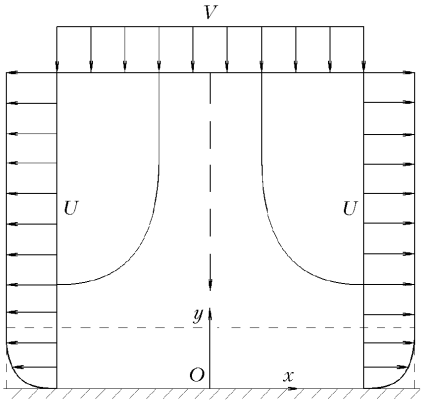

Fig. 1. Flow in the vicinity of the critical point.

curves merge together, whereas when $r_p < r_{p*}$ and $\vartheta_w < 1$ the $\zeta(r_p)$ the curves are stratified by the temperature parameter and deposition of the impurity on the wall is absent ($\zeta = 0$) for $\vartheta_w > 1$.

Stochastic simulation of the deposition of an impurity on cold and heated walls has been carried out in [4, 11]. In [4], the fluctuation field of the carrier-flow velocity is taken to be Gaussian, whereas in [11] experimental data are used to simulate it. The results obtained demonstrate a substantial influence of the migration mechanism [4, 11] and thermophoresis [7, 10] on the deposition of an impurity.

Whereas the theory of inertial deposition for $\mathrm{Stk} < \mathrm{Stk}_*$ predicts the absence of settling particles, experimental data show that in this case, too, there are particles arriving at the wall, and the fraction of small particles in deposits is much higher than that of large particles [7]. This can be due to the migration mechanism of motion and deposition of the impurity [4, 11].

In this work, we consider the problems of construction and numerical realization of the model of deposition of an impurity from a turbulent gas-dispersed flow in the vicinity of a critical point. The influence of the turbulence of the carrier flow on the behavior of the dispersed impurity is taken into account by introduction of random fluctuations of the velocity of a carrier medium into the equation of motion of a particle. The anisotropy of the turbulence field near the wall is allowed for on the basis of damping functions, to construct which we use experimental data. The equations describing the motion of the impurity are integrated in the known (computed in advance) gasdynamic field of a carrier gas (the back influence of particles on the gas is disregarded). We investigate the influence of the particle size and the initial parameters of the flow on the regularities of the scattering and deposition of the impurity near the critical point. The results of numerical simulation are compared within the framework of different models; the calculation results are compared to the data obtained without allowance for the influence of turbulent pulsations on the motion of particles.

Simulation of the Gas Phase. Let us consider plane or axisymmmetric flow of a mixture of a viscous heat-conducting gas with monodisperse condensed particles of a spherical shape near the critical point. We bring the x axis of a rectangular or cylindrical coordinate system into coincidence with the wall and guide the y axis perpendicularly to it. We locate the origin of the coordinate system at the critical point O (Fig. 1).

Change in the hydrodynamic situation in the immediate vicinity of the obstacle surface, in particular, the presence of a boundary layer and the influence of the temperature of the surface in flow, affects the process of deposition of an impurity most strongly.

For fairly high Reynolds numbers the flow region is subdivided into two subregions: the external region, where the viscosity and thermal conductivity of the gas are insignificant, and the internal region (thin boundary layer). Continuous fields of the parameters of the gas throughout the region are obtained by joining the solutions in the nonviscous region and in the boundary layer.

External Region. In the vicinity of the critical point, the components of the velocity of nonviscous potential flow have the form [12]

$$U = ax\,, \quad V = -(n+1)\,ay\,.$$

The velocity gradient of nonviscous flow in the direction $a = dU/dx$ (it is in parallel to the wall) represents the parameter of solution. In the vicinity of the critical point, we have $a = BV_\infty/L$, and the quantity B depends on the geometry of the obstacle ($B = 1$ for a plane plate, $B = 2$ for a circular cylinder, and $B = 3$ for a sphere).

In the external region of the boundary layer, the characteristics of turbulence are calculated on the basis of the following equations:

$$V\frac{dk}{dy} = -\varepsilon\,, \quad V\frac{d\varepsilon}{dy} = -c_{\varepsilon 2}\frac{\varepsilon^2}{k}\,.$$

Variation in the characteristics of turbulence along the longitudinal coordinate is disregarded [13]. Setting $V = V_\infty$, separating variables, and determining the integration constants from the boundary conditions, we obtain

$$\frac{k}{k_\infty} = \left[1 - (c_{\varepsilon 2} - 1)\frac{\varepsilon_\infty}{k_\infty V_\infty}(y_\infty - y)\right]^{1/(1-c_{\varepsilon 2})}, \quad \frac{\varepsilon}{\varepsilon_\infty} = \left(\frac{k}{k_\infty}\right)^{c_{\varepsilon 2}}.$$

The above relations determine the boundary conditions for calculation of the boundary layer.

Internal Region. The system of equations describing flow of a compressible gas in the turbulent boundary layer has the form [12]

$$\frac{\partial \rho u x^n}{\partial x} + \frac{\partial \rho v x^n}{\partial y} = 0\,, \tag{1}$$

$$\rho\left(u\frac{\partial u}{\partial x} + v\frac{\partial u}{\partial y}\right) = -\frac{dp}{dx} + \frac{\partial}{\partial y}\left[(\mu + \mu_t)\frac{\partial u}{\partial y}\right], \tag{2}$$

$$\rho c\left(u\frac{\partial T}{\partial x} + v\frac{\partial T}{\partial y}\right) = u\frac{dp}{dx} + \frac{\partial}{\partial y}\left[(\lambda + \lambda_t)\frac{\partial T}{\partial y}\right] + (\mu + \mu_t)\left(\frac{\partial u}{\partial y}\right)^2, \tag{3}$$

$$\rho\left(u\frac{\partial k}{\partial x} + v\frac{\partial k}{\partial y}\right) = \frac{\partial}{\partial y}\left[\left(\mu + \frac{\mu_t}{\sigma_k}\right)\frac{\partial k}{\partial y}\right] + \mu_t\left(\frac{\partial u}{\partial y}\right)^2 - \rho\varepsilon\,, \tag{4}$$

$$\rho\left(u\frac{\partial \varepsilon}{\partial x} + v\frac{\partial \varepsilon}{\partial y}\right) = \frac{\partial}{\partial y}\left[\left(\mu + \frac{\mu_t}{\sigma_\varepsilon}\right)\frac{\partial \varepsilon}{\partial y}\right] + c_{\varepsilon 1}\mu_t\frac{\varepsilon}{k}\left(\frac{\partial u}{\partial y}\right)^2 - c_{\varepsilon 2}\rho\frac{\varepsilon^2}{k}\,. \tag{5}$$

The pressure gradient dp/dx is found by solution of the nonviscous problem.

Equations (1)–(5) are supplemented with the equation of state of an ideal perfect gas $p = \rho RT$. Turbulent viscosity is computed from the Kolmogorov–Prandtl formula $\mu_t = c_\mu \rho k^2/\varepsilon$. We take the power-law dependence of the viscosity on temperature

$$\frac{\mu}{\mu_s} = \left(\frac{T}{T_s}\right)^m.$$

The boundary conditions for Eqs. (1)–(5) are formulated on the obstacle surface and in an unperturbed flow

$$u = v = k = \varepsilon = 0\,, \quad T = T_w \quad \text{for} \quad y = 0\,;$$

$$u = U\,,\quad T = T_\infty\,,\quad k = k_\infty\,,\quad \varepsilon = \varepsilon_\infty \quad \text{for} \quad y = \infty\,.$$

Calculation of the characteristics of viscous flow is complicated by the small thickness of the boundary layer and the large gradients of the functions sought in the region of interaction of the flow with the obstacle.

Transformation of Basic Equations. To obtain the coordinate system in which the gradients of the sought functions near the wall decrease and to eliminate the singularity occurring at the critical point we introduce transformation of the coordinates

$$\xi = \sqrt{\frac{a}{\nu_s}}\,x\,,\quad \eta = \sqrt{\frac{a}{\nu_s}}\,y\,.$$

We assume that, in the small vicinity of the critical point, the distributions of the velocity, pressure, temperature, and turbulence characteristics have the form

$$u = \sqrt{a\nu_s}\,\xi\varphi'(\eta)\,\vartheta(\eta)\,,\quad v = -(n+1)\sqrt{a\nu_s}\,\varphi(\eta)\,\vartheta(\eta)\,,$$

$$p_s - p = a\rho_s\nu_s\left[\xi^2/2 + \chi(\eta)\right],\quad T = T_s\vartheta(\eta)\,,$$

$$k = a\nu_s\psi(\eta)\,,\quad \varepsilon = a^2\nu_s\omega(\eta)\,.$$

Since we have $\partial p/\partial y = 0$ in the boundary layer, the density distribution at each point of x across the boundary-layer thickness is found in terms of the temperature distribution

$$\rho(\eta) = \frac{\rho_s}{\vartheta(\eta)}\,.$$

After the substitution of the above relations into Eqs. (1)–(5) and neglect of the terms of the order ξ^2 in the small vicinity of the critical point, we obtain the following system of equations:

$$\left[(\vartheta^m + \phi)(\varphi'\vartheta)'\right]' + (n+1)\,\varphi(\varphi'\vartheta)' - \vartheta\varphi'^2 + 1 = 0\,, \tag{6}$$

$$\left[\left(\frac{\vartheta^m}{\mathrm{Pr}} + \frac{\phi}{\mathrm{Pr}_t}\right)\varphi'\right]' + (n+1)\,\varphi\vartheta' = 0\,, \tag{7}$$

$$\left[\left(\vartheta^m + \frac{\phi}{\sigma_k}\right)\psi'\right]' + (n+1)\,\varphi\psi' - \frac{\omega}{\vartheta} = 0\,, \tag{8}$$

$$\left[\left(\vartheta^m + \frac{\phi}{\sigma_\varepsilon}\right)\omega'\right]' + (n+1)\,\varphi\omega' - c_{\varepsilon 2}\frac{\omega}{\psi\vartheta} = 0\,. \tag{9}$$

Here $\phi = \mu_t/\mu$.

In transformed variables, the following conditions will take the form

$$\varphi = \varphi' = \psi = \omega = 0\,,\quad \vartheta = \vartheta_w \quad \text{for} \quad \eta = 0\,;$$

$$\varphi' = 1\,, \quad \vartheta = 1\,, \quad \psi = \psi_\infty\,, \quad \omega = \omega_\infty \quad \text{for} \quad \eta = \infty\,.$$

The solution of Eqs. (6)–(9) is constructed on the basis of scalar and vector runs with iterational matching by nonlinearities and blocks of equations.

Simulation of the Dispersed Phase. Equations describing the translational motion of a spherically shaped particle have the form

$$\frac{d\mathbf{r}_\mathrm{p}}{dt} = \mathbf{v}_\mathrm{p}\,, \tag{10}$$

$$\frac{d\mathbf{v}_\mathrm{p}}{dt} = \frac{3C_\mathrm{D}\rho}{8\rho_\mathrm{p} r_\mathrm{p}} \left|\mathbf{v} - \mathbf{v}_\mathrm{p}\right| (\mathbf{v} - \mathbf{v}_\mathrm{p})\,. \tag{11}$$

The drag coefficient is computed using the relations of [14]. In addition to the drag force, we introduce into the model of interaction of the particle with the gas flow the Saffman lifting force and the thermophoresis force [15] which allow for the shearing character of flow in the boundary layer and the influence of the temperature of the surface in flow.

Equations (10) and (11) are integrated along the trajectory of an individual particle and require that only the initial conditions — the coordinates of the particle and its velocity at the instant of time $t = 0$ — be specified.

The gas velocity in the turbulent flow represents a random field of spatial coordinates and time. The influence of turbulence on the behavior of a particle is allowed for by introduction of random fluctuations of the velocity of the carrier medium into Eq. (11). The gas velocity is represented in the form of the sum of the average component and a random quantity that is selected within the framework of a locally isotropic and locally homogeneous approximation from the normal distribution law with a zero mathematical expectation and a standard deviation

$$\sigma = \sqrt{\frac{2}{3}k}\,.$$

The assumption on the isotropy of turbulence leads to an overstatement of the fluctuations of the velocity component normal to the wall [4, 5]. To allow for the anisotropy of flow we introduce the damping functions

$$f_i = \frac{\langle v_i' v_k' \rangle}{3I}\,.$$

The value of the random velocity component is computed from the formula

$$v_i' = \sigma f_i\,.$$

The damping functions are constructed on the basis of experimental data [16] according to which the maximum value of the pulsation of the velocity component normal to the wall exceeds approximately 2.4–2.6 times the corresponding value in the direction that is in parallel to the wall. Such an approach leads to more realistic results than the model of [4], which is based on the isotropic Gaussian random field of velocity fluctuations, and the model used in [3], in which the Kreichman model is used for calculation of velocity fluctuations.

The turbulence field is simulated by a set of spherical vortices of different size, and the sampled velocity fluctuation is assumed to be constant inside the vortex during its lifetime. As soon as the particle goes beyond the initial mole or the lifetime of the vortex elapses and it loses its individuality, a new fluctuation is sampled [17, 18]. The lifetime and size of the vortex to which the fluctuation is linked are determined by the local characteristics of turbulence.

As the time criterion of generation of a new fluctuation, we use the minimum from the lifetime of the vortex and the time of traversal of the vortex by the particle

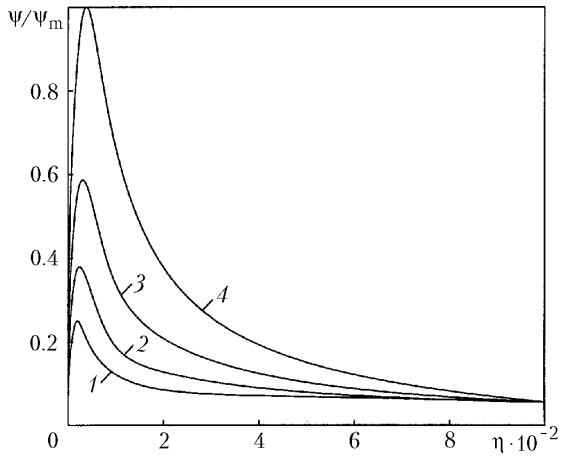

Fig. 2. Distribution of the kinetic turbulence energy in the vicinity of the critical point for $\theta\sqrt{\mathrm{Re}_\infty}$ = 20 and $\mathrm{Re}_\infty = 5\cdot10^4$ (1); 10^5 (2); $2\cdot10^5$ (3); $5\cdot10^5$ (4).

$$\Theta = \min\left\{\Theta_e, \Theta_c\right\} = \min\left(\frac{L_e}{\sqrt{2k/3}}, -\tau \ln\left(1 - \frac{L_e}{\tau\,|\mathbf{v} - \mathbf{v}_p|}\right)\right\}.$$

The time of dynamic relaxation of the particle is computed from the relation

$$\tau = \frac{8}{3}\frac{\rho}{\rho_p}\frac{r_p}{C_D\,|\mathbf{v} - \mathbf{v}_p|}.$$

If $L_e > \tau\,|\mathbf{v} - \mathbf{v}_p|$, the expression for Θ_c loses its meaning. This means that the particle does not go beyond the given vortex and remains within it as long as it exists. The time criterion of generation of a new fluctuation is assumed to be Θ_e.

The integral turbulence scale $L_e \sim k^{3/2}/\varepsilon$ is used as the space criterion.

Particular Cases. The formulated system of equations (6)–(9) enables us to generalize certain particular cases.

Nonviscous Approximation. For Stokes particles ($C_d = 24/\mathrm{Re}_p$), a distinctive feature of Eqs. (10) and (11) is that the equations describing particle motion in the longitudinal (axial) and transverse (radial) directions are integrated in finite form independently of one another [6].

The pattern of motion of the impurity is determined by the Stokes number. It is convenient to introduce a modified Stokes number $S = B\,\mathrm{Stk}$ whose critical value $S_* = 0.25/(n+1)$ is independent of the geometry of the obstacle. When $S < S_*$, the particles do not reach the surface in finite time. When $S > S_*$, the particles that move in equilibrium with the gas at a certain initial distance from the critical point always collide with the wall.

The dependence of the sedimentation coefficient on the Stokes number, calculated for nonseparating potential flow past the obstacle, is the lower bound for the sedimentation coefficient under actual conditions, for example, with allowance for gravitational effects or for the temperature of the surface in flow [7].

Influence of the Boundary Layer. The equations describing the velocity and temperature distributions in the laminar boundary layer of an incompressible liquid are obtained from Eq. (6)–(9) for $\vartheta \equiv 1$ and $\phi \equiv 1$ and coincide with the Folkner–Scan equations [12]. The dynamic and thermal problems are separated and the equation of variation of the temperature is solved with the known velocity distribution.

In this case the pattern of motion of the impurity is determined by the Reynolds and Stokes numbers. For high Reynolds numbers the boundary-layer thickness is small; consequently, the distance traversed by the particles in the boundary layer and the work done by the gas on the particles are also small. The boundary layer exerts a substantial influence on the final stage of deposition of fairly small particles incident on the wall at a large angle [6]. Allowance for the boundary layer leads to an increase in the critical Stokes number [7, 19]. Langmiur formulas are used to evaluate the coefficient of sedimentation of the impurity on the surface of a sphere [15].

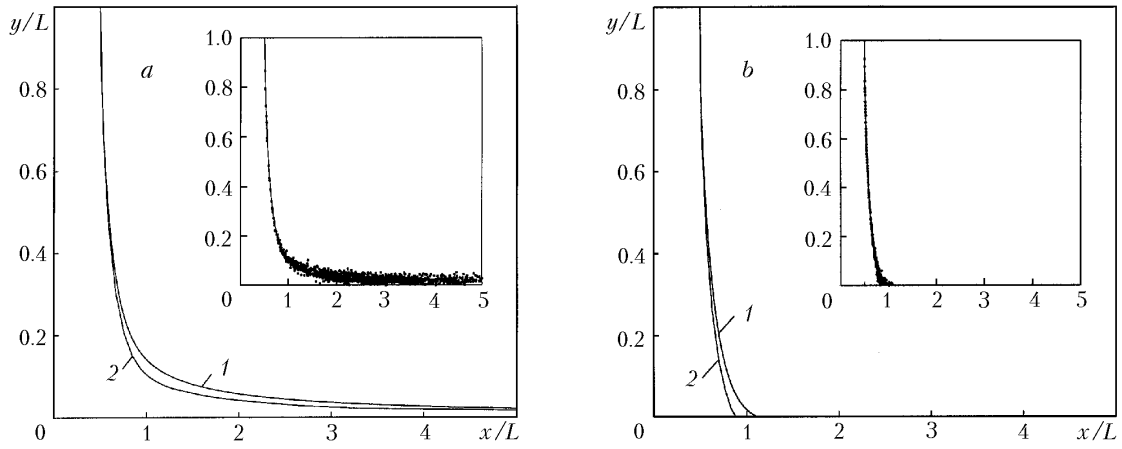

Fig. 3. Trajectory of motion of a particle of radius r_p = 5 μm (a) and r_p = 15 μm (b) in the region of interaction of the flow with the obstacle with neglect of (curves 1) and allowance for (curves 2) the turbulent pulsations of the carrier flow. The insets show realizations of the random trajectories of notion of the particles.

In the diffusion approximation, when Fick's law is taken for the rate of diffusion of the impurity, the equation for the concentration of the dispersed phase is reduced to an ordinary differential equation of second order whose solution is obtained in finite form [20].

Influence of the Nonisothermality of Flow. The equations describing the velocity and temperature distributions in the laminar boundary layer of a compressible liquid are obtained for $\phi \equiv 0$. Allowance for the nonisothermality and compressibility of flow cause the velocity field to become dependent on the temperature of the surface in flow (the dynamic and thermal problems are interrelated).

In the nonisothermal flow, the characteristics of deposition are affected by the temperature factor in addition to the Reynolds and Stokes numbers. The influence of the wall temperature on the deposition of an impurity is considered in [7, 10]. Deposition of small particles under nonisothermal conditions is determined by the action of a thermophoretic force causing the displacement of the particles in the direction opposite to the temperature gradient.

Influence of Turbulence. The equations describing turbulent flow of an incompressible liquid in the vicinity of the critical point are obtained for $\vartheta \equiv 1$ and are given in [21] (including the cases allowing for the back influence of the impurity).

The calculation results demonstrate a sharp increase in the pulsation characteristics of the flow in the wall viscous region of flow (Fig. 2). They are normalized to the maximum value of the kinetic turbulence energy $\psi_m = 3.8 \cdot 10^3$ at $\mathrm{Re}_\infty = 5 \cdot 10^5$. Turbulent pulsations of the carrier flow are observed in the immediate vicinity of the entrainment surface, and the turbulent-migration mechanism is of primary importance in the deposition of the impurity.

Results and Discussion. Let us consider the regime of inertial deposition where all incident particles are absorbed by the surface. The intensity of deposition of the particles is characterized by the sedimentation coefficient by which we mean the ratio of the density of the flux of incident particles at the critical point to the density of the flux of particles of a given fraction in an unperturbed flow. The sedimentation coefficient is computed from the formula

$$\zeta = \left(\frac{x_{p0}}{x_{p,w}} \right)^{n+1} .$$

Its calculation requires that the trajectory of a particle passing through a certain point x_{p0} in the unperturbed flow and meeting with the surface at the point $x_{p,w}$ be known.

Some results of numerical calculations on deposition of alumina particles from a turbulent air flow on a sphere are given in Figs. 3 and 4. The parameters of the gas and dispersed phases are as follows: V_∞ = 1–30 m/sec, T_∞ = 273 K, $k_\infty = 10^4$–10^{-1} m^2/sec^2, $\varepsilon_\infty = 10^4$–$10^{-1}$ m^2/sec^2, L = 1 m, r_p = 1–50 μm, u_{p0} = 0, $v_{p0} = V_\infty$, x_{p0}/L =

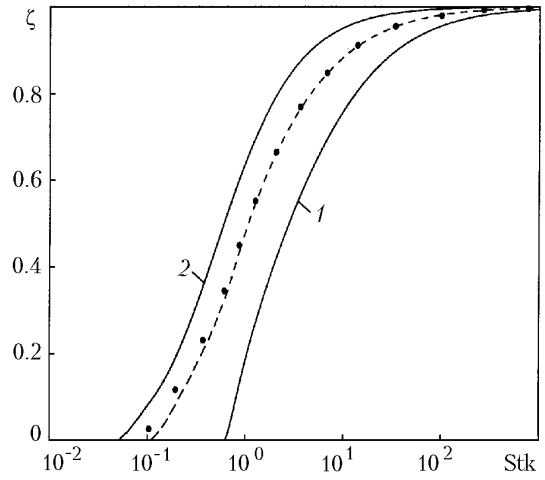

Fig. 4. Coefficient of sedimentation of the impurity on the surface of a sphere vs. particle size: 1 and 2) models of creeping and nonviscous flow near the sphere; dashed curve, results of calculation at $Re_\infty = 10^5$ without allowance for the influence of the fluctuations of the carrier-flow velocity; dots, results of calculation according to the stochastic model.

0.5, y_{p0}/L = 5.0, Pr = 0.72, and m = 0.76. The thermophysical properties of the gas and the particles have been taken from the reference literature.

The trajectories of particles of prescribed size are constructed at a fixed value of y_{p0} and with variation of the value of x_{p0} with a certain step from 0 to the value of $x_{p,w}$ for which the condition of arrival of a particle at the surface in flow is not observed. The particle contacting the obstacle surface is assumed to be the condition of deposition of the particle on the obstacle. The coordinate of the point of contact is taken as the deposition coordinate $x_{p,w}$.

To describe the behavior of the impurity in the turbulent flow on the basis of the stochastic model we must calculate the trajectories of a large number of trial particles. In the calculations, we simulated from 10^3 to 10^4 trajectories of trial particles depending on their size. The integration step along each trajectory was bounded by the time and space scales of turbulence. The decrease in the particle size leading to an increase in the number of realizations is necessary for obtaining a statistically reliable average pattern of motion of the impurity due to the growth in the contribution of the interactions of a particle with vortices of progressively smaller size.

The trajectories of particle motion in the region of interaction of the flow with the obstacle are shown in Fig. 3a (subcritical Stokes number, Stk = 0.0312) and in Fig. 3b (supercritical Stokes number, Stk = 0.1097). Curves 1 correspond to the results obtained without allowance for the influence of turbulent pulsations on the motion of a particle, whereas curves 2 correspond to the results of statistical averaging over the ensemble of particles.

At a large distance from the obstacle surface, the trajectories of particles represent straight lines. As the obstacle is approached, the trajectories of small particles ($r_p < 8$ μm) bend similarly to the streamlines of the liquid (Fig. 3a); part of the particles does not reach the surface (when $Stk < Stk_*$).

In the nonviscous region, the gradients of kinetic turbulence energy are small; therefore, the effect of turbophoresis is slight here. The influence of turbulent velocity pulsations on the motion of a particle begins to appear upon its arrival at the wall region. The inhomogeneity of the turbulence field of the gas phase in the presence of the maximum of kinetic energy in the boundary layer gives rise to the particle's turbulent migration (turbophoresis force) directed toward decreasing pulsation energy of the gas (to the wall). For particles of large fractions ($r_p < 12$ μm), the boundary layer and the velocity pulsations in it exert no substantial influence on the motion and scattering of the impurity by virtue of the inertia of such particles (Fig. 3b).

The dependences of the sedimentation coefficient on the particle size that have been obtained within the framework of different models are shown in Fig. 4. Curves 1 and 2 correspond to the models of creeping ($Re_\infty \to 0$ and $Stk_* = 0.6070$) and nonviscous ($Re_\infty \to \infty$ and $Stk_* = 0.0417$) flows near the sphere. Allowance for the turbulent fluctuations of the carrier-flow velocity leads to higher values of the sedimentation coefficient (dots) than those in the

case where the fluctuations are disregarded (dashed curve). The migration mechanism of motion of the impurity in the turbulent boundary layer contributes to the additional deposition of small particles. Furthermore, the influence of the relative velocity of motion of the phases (particles keep ahead of the gas) should be taken into account in the boundary layer.

Under nonisothermal conditions, the dependence of the sedimentation coefficient on the Stokes number is basic in the region $\mathrm{Stk} > \mathrm{Stk}_*$, where the inertial mechanism of deposition is dominant. In the region of small particles ($\mathrm{Stk} < \mathrm{Stk}_*$), the influence of the Stokes number is ambiguous. As the Stokes number increases, the sedimentation coefficient can increase or decrease depending on the parameter due to which Stk changes. For example, the sedimentation coefficient monotonically drops with variation of it due to the increase in V_∞ and r_p and monotonically increases with variation due to the decrease in L.

The Saffman force affects the intensity of deposition of the impurity but rather slightly, particularly under isothermal conditions. The main contribution to the increase in the sedimentation coefficient in the turbulent flow is made by the migration coefficient.

CONCLUSIONS

The investigations carried out have shown that the migration mechanism exerts a substantial influence on the motion and deposition of the impurity in the vicinity of the critical point. The constructed model leads to satisfactory results consistent with the data of numerical experiments within the framework of different models. The use of the migration model allowing for the dispersion of the impurity in the turbulent flow makes it possible, in particular, to explain the removal of particles to the obstacle's surface and the presence of dispersed-phase deposits in the case where the Stokes number turns out to be lower than its critical value.

Further development of the model involves the abandonment of damping functions allowing for the anisotropy of the turbulence field in the boundary layer and the application of the equations of transport of Reynolds stresses, direct numerical simulation, and the method of simulation of large vortices to the calculation of the flow parameters.

NOTATION

a, gradient of the velocity of nonviscous flow, 1/sec; c, specific heat at constant pressure, J/(kg·K); c_μ, $c_{\varepsilon 1}$, and $c_{\varepsilon 2}$, constants of the turbulence model; f, damping function; k, kinetic turbulence energy, $\mathrm{m}^2/\mathrm{sec}^2$; m, exponent in the dependence of the viscosity on temperature; n, index of the geometry of flow; p, pressure, Pa; r, radius, m; $\mathbf{r}$, radius vector, m; t, time, sec; u and v, components of the velocity of viscous flow, m/sec; $\mathbf{v}$, velocity vector, m/sec; x and y, longitudinal and transverse coordinates, m; B, parameter dependent on the geometry of the obstacle; C_d, drag coefficient of a particle; L, characteristic space scale, m; Pr, Prandtl number; R, gas constant, J/(kg·K); Re, Reynolds number; S, modified Stokes number; Stk, Stokes number; T, temperature, K; U and V, components of the velocity of nonviscous potential flow, m/sec; ε, rate of dissipation of turbulent energy, $\mathrm{m}^2/\mathrm{sec}^3$; ζ, sedimentation coefficient; ϑ, dimensionless temperature; λ, thermal conductivity, W/(m·K); μ, dynamic viscosity, $\mathrm{N}/(\mathrm{m}^2\cdot\mathrm{sec})$; ν, kinematic viscosity, $\mathrm{m}^2/\mathrm{sec}$; ξ and η, self-similar constants; θ, degree of turbulence; ρ, density, kg/m^3; σ, standard deviation; σ_k and σ_ε, constants of the turbulence model; τ, dynamic-relaxation time, sec; ϕ, φ, χ, ψ, and ω, dimensionless turbulent viscosity, velocity, pressure, kinetic energy of turbulence, and rate of dissipation of turbulence energy; Θ, characteristic time scale, sec. Subscripts and superscripts: c refers to the time of traversal of the vortex by a particle; e, turbulent vortex (eddy); i, tensor index; m, maximum; p, particle; s, critical (stagnation) point; t, turbulent; w, wall; 0, refers to the parameters at the initial instant of time; ∞, infinity; *, critical value of the parameter; $'$, refers to the pulsatory parameters of the flow; d refers to the characteristics of drag of a particle.

REFERENCES

1. E. P. Mednikov, *Turbulent Transfer and Precipitation of Aerosols* [in Russian], Nauka, Moscow (1981).
2. M. Shin, D. S. Kim, and J. W. Lee, Deposition of inertia-dominated particle inside a turbulent boundary layer, *Int. J. Multiphase Flow*, **29**, No. 1, 893–926 (2003).

3. Q. Chen and G. Ahmadi, Deposition of particles in a turbulent pipe flow, *J. Aerosol Sci.*, **28**, No. 5, 789–796 (1997).
4. C. Kroger and Y. Drossions, A random-walk simulation of thermophoretic particle deposition in a turbulent boundary layer, *Int. J. Multiphase Flow*, **26**, 1325–1350 (2000).
5. E. A. Matida, K. Nishino, and K. Torii, Statistical simulation of particle deposition on the wall from turbulent dispersed pipe flow, *Int. J. Heat Fluid Flow*, **21**, 389–402 (2000).
6. J. A. Laitone, Erosion prediction near a stagnation point resulting from aerodynamically entrained solid particles, *J. Aircraft*, **16**, No. 12, 809–814 (1979).
7. F. E. Spokoinyi and Z. R. Gorbis, Special features of deposition of fine-dispersed particles from a cooled gas flow on a transversely streamlines heat-transfer surface, *Teplofiz. Vys. Temp.*, **19**, No. 1, 182–199 (1981).
8. A. N. Osiptsov, Boundary layer on a blunt body in dusted gas flow, *Izv. Akad. Nauk SSSR, Mekh. Zhidk. Gaza*, No. 5, 99–107 (1985).
9. A. P. Vasil'kov, Vicinity of the critical point of a blunt body in the hypersonic two-phase flow, *Izv. Akad. Nauk SSSR, Mekh. Zhidk. Gaza*, No. 5, 121–129 (1975).
10. Yu. M. Tsirkunov and N. V. Tarasova, Influence of the temperature of the obstacle on deposition of impurity from a supersonic gas-suspension flow, *Teplofiz. Vys. Temp.*, **30**, No. 6, 1154–1162 (1992).
11. C. Greenfield and G. Quarini, A Lagrangian simulation of particle deposition in a turbulent boundary layer in the presence of thermophoresis, *Appl. Math. Model.*, **22**, 759–771 (1998).
12. H. Schlichting, *Boundary Layer Theory* [Russian translation], Nauka, Moscow (1974).
13. R. M. Traci and D. C. Wilcox, Freestream turbulence effects on stagnation point heat transfer, *Raketn. Tekh. Kosmonavt.*, **13**, No. 7, 61–69 (1975).
14. C. B. Henderson, Drag coefficients of spheres in continuum and rarefied flows, *AIAA J.*, **14**, No. 6, 707–708 (1976).
15. L. E. Sternin and A. A. Shraiber, *Multiphase Particle-Laden Gas Flows* [in Russian], Mashinostroenie, Moscow (1994).
16. Y. Guo nd D. H. Wood, Measurements in the vicinity of a stagnation point, *Exp. Thermal Fluid Sci.*, **25**, 605–614 (2002).
17. A. D. Gosman and E. Ioannides, Aspects of Computer Simulation of Liquid-Fuel Combustors, *AIAA Paper*, No. 81-0323 (1981).
18. K. N. Volkov and V. N. Emel'yanov, A stochastic model of motion of a condensed particle in a channel with permeable walls, *Mat. Modelir.*, **11**, No. 3, 105–111 (1999).
19. C. G. Phillips and S. R. Kaye, The influence of the viscous boundary layer on the critical Stokes number for particle impaction near a stagnation point, *J. Aerosol Sci.*, **30**, No. 6, 709–718 (1999).
20. R. Tsai and L. J. Liang, Inertial effect on aerosol particle deposition from an axisymmetric stagnation point flow approximation, *Int. Commun. Heat Mass Transfer*, **29**, No. 4, 489–496 (2002).
21. K. N. Volkov and V. N. Emel'yanov, Calculation of turbulent two-phase flow in the region of impingement of a flow on a body, *Inzh.-Fiz. Zh.*, **71**, No. 4, 599–605 (1998).